The Journal of Toxicological Sciences (J. Toxicol. Sci.)
Vol.45, No.6, 349-363, 2020

Original Article

Redox cycling of 9,10-phenanthrenequinone activates epidermal growth factor receptor signaling through *S*-oxidation of protein tyrosine phosphatase 1B

Nho Cong Luong[1,2,*], Yumi Abiko[1,3,*], Takahiro Shibata[4], Koji Uchida[4,5], Eiji Warabi[1,3], Midori Suzuki[6], Takuya Noguchi[6], Atsushi Matsuzawa[6] and Yoshito Kumagai[1,3]

[1]Doctoral Program in Biomedical Sciences, Graduate School of Comprehensive Human Sciences, University of Tsukuba, Tsukuba, Ibaraki 305-8575, Japan
[2]Faculty of Pharmacy, Hue University of Medicine and Pharmacy, Hue University, 06 Ngo Quyen, Hue, Vietnam
[3]Faculty of Medicine, University of Tsukuba, Tsukuba, Ibaraki 305-8575, Japan
[4]Graduate School of Bioagricultural Sciences, Nagoya University, Nagoya, Aichi 464-8601, Japan
[5]Graduate School of Agricultural and Life Sciences, The University of Tokyo, Tokyo 113-8657, Japan
[6]Graduate School of Pharmaceutical Sciences, Tohoku University, Sendai, Miyagi 980-8578, Japan

(Received March 24, 2020; Accepted April 19, 2020)

ABSTRACT — 9,10-Phenanthrenequinone (9,10-PQ) is a polycyclic aromatic hydrocarbon quinone contaminated in diesel exhaust particles and particulate matter 2.5. It is an efficient electron acceptor that induces redox cycling with electron donors, resulting in excessive reactive oxygen species and oxidized protein production in cells. The current study examined whether 9,10-PQ could activate epidermal growth factor receptor (EGFR) signaling in A431 cells through *S*-oxidation of its negative regulators such as protein tyrosine phosphatase (PTP) 1B. 9,10-PQ oxidized recombinant human PTP1B at Cys215 and inhibited its catalytic activity, an effect that was blocked by catalase (CAT), whereas *cis*-9,10-dihydroxy-9,10-dihydrophenanthrene (DDP), which lacks redox cycling activity, had no effect on PTP1B activity. Exposure of A431 cells to 9,10-PQ, but not DDP, activated signaling through EGFR and its downstream extracellular signal-regulated kinase 1/2 (ERK1/2), coupled with a decrease of cellular PTP activity. Immunoprecipitation and UPLC-MS^E revealed that PTP1B easily undergoes oxidation during exposure of A431 cells to 9,10-PQ. Pretreatment with polyethylene glycol conjugated with CAT (PEG-CAT) abolished 9,10-PQ–generated H_2O_2 production and significantly blocked the activation of EGFR-ERK1/2 signaling by 9,10-PQ, indicating the involvement of H_2O_2 in the activation because scavenging agents for hydroxyl radicals had no effect on the redox signal activation. These results suggest that such an air pollutant producing H_2O_2, activates EGFR-ERK1/2 signaling, presumably through the *S*-oxidation of PTPs such as PTP1B, and activation of the signal cascade may contribute, at least in part, to cellular responses in A431 cells.

Key words: 9,10-Phenanthrenequinone, Reactive oxygen species, Redox signaling, Epidermal growth factor receptor, Protein tyrosine phosphatases, Hydrogen peroxide

INTRODUCTION

Post-translational modification of proteins through reactive cysteine (Cys) residues plays a crucial role in maintaining intracellular homeostasis. The current consensus is that sensor proteins (e.g., phosphatases) with low p*K*a Cys thiols (P-SH), which are predominantly deprotonated to form thiolate ions (P-S$^-$) at physiological pH, are targets of oxidative and covalent modification by reactive oxygen species (ROS) and electrophiles, thereby leading to activation of their effector molecules (e.g., kinases, transcription factors) (Rudolph and Freeman, 2009; Marnett *et al*., 2003; Jones, 2008). Such oxidation and reduction of sensor proteins regulate redox signal pathways to maintain cellular homeostasis. Protein tyrosine phosphatases (PTPs) are sensor proteins with HCX_5R(S/T) motifs in their active sites (Zhang, 1998). Because the Cys in the active site has a lower p*K*a (e.g.,

Correspondence: Yoshito Kumagai (E-mail: yk-em-tu@md.tsukuba.ac.jp)
*These authors equally contributed to this work.

5.4 for PTP1B) because of its interaction with hydrogen bond donors in the unique surrounding environment (Lohse *et al*., 1997; Zhang and Dixon, 1993; Zhang, 2003), ROS readily oxidize Cys to sulfenic acid (P-SOH). Endogenous H_2O_2 produced by the epidermal growth factor (EGF)-mediated activation of NADPH oxidases transiently inhibits PTP activity through the oxidation of thiols PTPs, thereby activating EGF receptor (EGFR) signaling, which is involved in cell survival and proliferation (Lee *et al*., 1998; Tiganis, 2002; Bae *et al*., 1997). The P-SOH is reported to convert sulfenylamide intermediate and/or P-SSG adduct that are able to back to original $P\text{-}S^-$ by glutathione or Cys-containing redox system such as thioredoxin (Trx) system (Seth and Rudolph, 2006; van Montfort *et al*., 2003; Dagnell *et al*., 2013; Barrett *et al*., 1999). However, H_2O_2 at excessive levels further oxidizes P-SOH to form irreversible oxidation-state sulfinic acid ($P\text{-}SO_2H$) followed by sulfonic acid ($P\text{-}SO_3H$) (Dickinson and Chang, 2011). It is reported that organic hydroperoxides inactivate PTP1B through oxidation (Bhattacharya *et al*., 2008) and lipophilic nitro-benzoxadiazole compounds are associated with dimerization of Cu,Zn-SOD to enhance intracellular production of H_2O_2 (Sakanyan *et al*., 2016). These suggest that exogenous ROS generators can also activate redox signaling following oxidative modification of thiol groups on the sensor.

Our previous study found that 9,10-phenanthrenequinone (9,10-PQ), a polycyclic aromatic hydrocarbon quinone present in diesel exhaust particles and particulate matter 2.5 (Cho *et al*., 2004; Chung *et al*., 2006), without covalent binding capability to protein thiols (Kumagai *et al*., 2002; Rodriguez *et al*., 2004, 2005), is an effective electron acceptor that undergoes redox cycling with electron donors. NADPH-dependent enzymes such as AKR1C and TrxR reduce 9,10-PQ to yield 9,10-dihydroxy-phenanthrene (9,10-PQH_2), which comproportionates with 9,10-PQ to form its semiquinone radical (9,10-$PQ^{\bullet-}$) (Taguchi *et al*., 2008, 2007; Cenas *et al*., 2004). 9,10-$PQ^{\bullet-}$ is also formed via the one-electron reduction of 9,10-PQ by dithiols, persulfides, or polysulfides (Kumagai *et al*., 2002; Abiko *et al*., 2019). 9,10-$PQ^{\bullet-}$ readily interacts with molecular oxygen to yield 9,10-PQ and superoxide ($O_2^{\bullet-}$), the latter of which reacts with 9,10-PQH_2 to generate H_2O_2 and 9,10-$PQ^{\bullet-}$ (Taguchi *et al*., 2008, 2007). H_2O_2 oxidizes ferrous ions to ferric ions and generates hydroxyl radical ($^{\bullet}OH$), which is the ultimate oxidant (Sugimoto *et al*., 2005). Through redox cycling, 9,10-PQ generates excessive amount of ROS in cell-free systems as well as in A549 cells (Taguchi *et al*., 2007, 2008; Kumagai *et al*., 2002; Sugimoto *et al*., 2005). Exposure of A549 cells to 9,10-PQ causes ROS overproduction, leading to protein oxidation and subsequent apoptotic cell death (Taguchi *et al*., 2007; Sugimoto *et al*., 2005). From these observations, we speculated that ROS such as H_2O_2 generated by 9,10-PQ could activate redox signaling pathways, leading to cytoprotective responses. In the present study, we investigated whether 9,10-PQ, as a model exogenous ROS generator through its redox cycling, activates EGFR-ERK1/2 signaling through the *S*-oxidation of PTPs.

MATERIALS AND METHODS

Materials

9,10-PQ (99% purity determined by HPLC), dimedone, EGF, *p*-nitrophenyl (*p*NP) phosphate (*p*NPP), catalase (CAT), and dimethyl sulfoxide (DMSO) were obtained from Sigma-Aldrich (St. Louis, MO, USA). 1,2-Naphthoquinone (NQ, 95% purity determined by HPLC) and 1,10-phenanthroline were purchased from Tokyo Chemical Industry (Tokyo, Japan). PD153035 and anti-PTP1B antibody (# PH01) were acquired from Calbiochem (San Diego, CA, USA). 3-(4,5-dimethyl-2-thiazolyl)-2,5-diphenyl-2H-tetrazolium bromide (MTT) was obtained from Dojindo Laboratories (Kumamoto, Japan). Anti-EGFR antibody (#2232), anti-phospho EGFR Tyr1068 antibody (#2234), anti-p44/42 MAP kinase antibody [anti-extracellular signal-regulated kinase 1/2 (ERK1/2), #9102], anti-phospho ERK1/2 antibody (#9101), horseradish peroxidase-linked anti-rabbit IgG (#7074), and anti-mouse IgG (#7076) secondary antibody were procured from Cell Signaling Technology (Beverly, MA, USA). Anti-sulfenic acid-modified antibody (2-thiodimedone–specific Ig, #ABS30) was purchased from Merck Millipore (Temecula, CA, USA). Anti-oxidized PTP active site (oxPTP) antibody (#MAB2844), which could specifically recognize sulfonic acid in the PTPs signature motif [$HC_{SO3H}X_5R(S/T)$] (Persson *et al*., 2004, 2005), was acquired from R&D Systems (Bio-techne, Minneapolis, MN, USA). Ni-IDA ProBond was purchased from Invitrogen (Carlsbad, CA, USA). HYDROP was obtained from Goryo Chemical (Hokkaido, Japan). Dithiothreitol (DTT) and H_2O_2 were procured from Wako Pure Chemical Industries (Osaka, Japan). Polyethylene glycol conjugated with CAT (PEG-CAT) was prepared as described previously (Sun *et al*., 2006). All other reagents used were of the highest purity available. Chemical structures were drawn using MarvinSketch version 17.3.27.0 (https://www.chemaxon.com).

Preparation of recombinant PTP1B protein

Recombinant human PTP1B (hPTP1B) was prepared as previously described (Iwamoto *et al*., 2007). Briefly, *E. coli* BL21 cells, which were transformed with a plasmid containing the isolated catalytic domain of human 37-kDa PTP1B (NH_2-terminal 321 residues) in a pET15b vector, were preincubated in LB broth containing 100 μg/mL ampicillin at 37°C with shaking overnight at 120 rpm. The bacteria were then large-scale cultured and grown to an absorbance of 0.6–0.8 at 600 nm. The protein was induced by the addition of 200 μM isopropyl-1-thio-β-D-galactopyranoside and incubated at 15°C with shaking at 120 rpm for an additional 21 hr. After harvesting by centrifugation, the cells were suspended in lysis buffer containing 50 mM Tris-HCl (pH 7.5), 100 mM NaCl, 10 mM 2-mercaptoethanol (2-ME), and 5% glycerol and sonicated on ice for 30 min. The sonicate was centrifuged at 105,398 × *g* for 1 hr to collect the supernatant, which was next applied to a Ni-IDA ProBond column at 4°C. The column was extensively washed with a buffer containing 50 mM Tris-HCl (pH 7.5), 100 mM NaCl, and 10 mM 2-ME. PTP1B was then eluted with imidazole in a linear gradient from 0 to 100 mM. The collected fractions were monitored by measuring the absorbance at 280 nm and SDS-PAGE. The fractions containing hPTP1B were reduced via incubation with 10 mM DTT for 1 hr on ice, and the low-molecular-weight compounds were removed using an Econo-Pac 10 DG column (Bio-Rad, Hercules, CA, USA). The protein concentration was determined using the Bio-Rad protein assay (Bio-Rad) based on the Bradford method (Bradford, 1976) according to the manufacturer's protocol. Purified PTP1B was stored at −80°C in 20 mM Tris-HCl (pH 7.5)–10 mM DTT, in which DTT was removed before use using centrifugal filters (Amicon Ultra 3K, Merck Millipore).

Phosphatase assay

The phosphatase assay using *p*NPP as a phosphatase substrate was performed as previous described (Iwamoto *et al*., 2007) with slight modifications. Briefly, A431 cells were exposed to the indicated compounds for 30 min. After washing with ice-cold phosphate-buffered saline (PBS), the cells were collected and lysed in RIPA buffer [50 mM Tris-HCl (pH 8.0), 0.1% SDS, 50 mM NaCl, 1% Nonidet P-40, and 0.5% deoxycholate] containing 1 μM okadaic acid (Merck Millipore), which is an inhibitor of serine/threonine-specific protein phosphatase (Cohen *et al*., 1989). The cell lysates (50 μg) were incubated with 10 mM *p*NPP–50 mM Tris-HCl (pH 7.5)–100 mM NaCl–0.1 mg/mL BSA–0.5% Tween 20 in the absence and presence of 10 mM DTT for 20 min at 37°C. The reaction was terminated by adding an equal volume of 2 M NaOH. The absorbance of the released *p*NP was determined at 405 nm using a spectrophotometer.

For hPTP1B, the protein [0.5 μg/μL in 50 mM Tris-HCl (pH 7.5)–0.1 mM EDTA] was incubated with the indicated compounds at 25°C for the indicated times. Then, aliquots containing 0.5 μg of PTP1B were reacted with 4 mM *p*NPP in 0.1 mM EDTA–100 mM acetate buffer (pH 5.5) for 10 min at 25°C. The reaction was terminated by adding an equal volume of 2 M NaOH, and the absorbance of *p*NP was measured at 405 nm.

Recombinant hPTP1B modification and UPLC-MS^E analysis

hPTP1B (13.5 μM) containing 1.25 mM DTT was incubated with 9,10-PQ at 25°C, followed by treatment with 5 mM dimedone for 1 hr. Then, low-molecular-weight compounds in the reaction mixture were removed using centrifugal filters (Amicon Ultra 3K, Merck Millipore). Dimedone-labeled SOH and SO_3H on the PTP1B active site in the samples were detected via Western blotting with anti-2-thiodimedone–specific antibody and oxPTP antibody, respectively.

For ultra-performance liquid chromatography-elevated collision energy mass spectrometry (UPLC-MS^E) analysis, the samples were incubated with 5 mM DTT in 50 mM ammonium bicarbonate buffer for 10 min at 25°C, followed by alkylation by adding 5 mM 2-iodoacetamide (IAA) for 20 min at 25°C in dark. After the reaction, the protein was digested using MS-grade modified trypsin (10 ng/μL; Promega, Madison, WI, USA) at 37°C overnight. UPLC-MS^E was performed using a nanoAcquity UPLC-MS^E system (Waters, Milford, MA, USA) equipped with a BEH130 nanoAcquity C_{18} column (100 mm × 75 μm i.d., 1.7 μm, Waters) and maintained at 35°C. Mobile phases (A, 0.1% formic acid in water; B, 0.1% formic acid in acetonitrile) at a flow rate of 0.3 μL/min were linearly mixed in a gradient program as follows: 3% B for 1 min; linear increase over 74 min to 40% B, maintained for 4 min; linear increase over 1 min to 95% B, maintained for 5 min before returning linearly to 3% B over 1 min. The total run time including conditioning of the column at the initial conditions was 100 min. The eluted peptides were directly transferred to the nano-electrospray source of a mass spectrometer (Synapt high definition Q-TOF, Waters) through a Teflon capillary union and a precut PicoTip (Waters). The initial parameters of the mass spectrometer were a capillary voltage of 2.5 kV and a sampling cone voltage of 35 V. The source temperature was 100°C, and the detector was operated in the positive ion mode. Low collision energy (6 eV) and

elevated collision energy (stepped from 15 to 30 eV) were used to generate intact peptide precursor ions and peptide product ions, respectively. MassLynx version 4.1 software (Waters) was used to control the system and analyze the mass spectral data. The MS survey scan range was *m/z* 300–2000 Da. The data were collected in the centroid mode and acquired using an independent reference. Glu-1-fibrinopeptide B (*m/z* 785.8426), which was used as an external mass calibration, was infused via the nanoLock-Spray ion source and sampled every 10 s. BiopharmaLynx version 1.2 software (Waters) was used to perform baseline subtraction, smoothing, and deisotoping to identify *de novo* peptide sequences and perform a database search.

Synthesis of cis-9,10-dihydroxy-9,10-dihydrophenanthrene (DDP)

9,10-PQ was added at a 100-fold molar excess to sodium tetrahydroborate (Wako) in ethanol in a final volume of 200 mL. After incubation with stirring for 1 hr at room temperature, the reduction was stopped by adding acetic acid, and ethanol was removed *in vacuo*. The residue was dissolved in water and extracted using chloroform. After removing chloroform *in vacuo*, the residue was separated using silica gel (YMC*GEL SIL, 6 nm pore size, 210 μm particle size, YMC, Kyoto, Japan) with chloroform/methanol (97/3, v/v) as the mobile phase. Each fraction was monitored via thin-layer chromatography and UPLC-MS^E analysis. The fractions containing the purified product of *m/z* 211.1 in the negative ion mode were collected and then recrystallized from solvent to yield a white powder. NMR spectroscopy (AVANCE400, Bruker, Billerica, MA, USA) identified the purified compound as follows: ^{1}H NMR (400 MHz, CD_3OD), δ 7.798 (d, 1H), δ 7.615 (d, 1H), δ 7.35 (m, 2H), δ 4.61 (s, 1H); ^{13}C NMR (100 MHz, CD_3OD), δ 139.161, δ 134.877, δ 130.134, δ 129.863, δ 128.431, δ 125.378, δ 75.114 (Fig. S1).

Cell culture

Human epithelial carcinoma cells (A431 cells, RIKEN Cell Bank, Ibaraki, Japan) are known as a useful model for studying EGFR downstream signaling because they highly express EGFR (Gamou *et al*., 1984). The cells were cultured in a 5% CO_2 humidified atmosphere at 37°C in Dulbecco's modified Eagle's medium (DMEM) supplemented with 10% fetal bovine serum, antibiotics (100 U/mL penicillin and 100 μg/mL streptomycin), and 2 mM glutaMAX-I. For each experiment, A431 cells were grown in proper dishes until reaching 80–100% confluence and then starved in serum-free DMEM for 24 hr before treatment with the indicated compounds.

Western blotting

After treatment, the cells were washed three times with ice-cold PBS and collected by scraping into lysis buffer [20 mM Tris-HCl (pH 7.5), 150 mM NaCl, 1 mM EDTA, 1 mM EGTA, 1% Triton X-100, 2.5 mM sodium pyrophosphate, 1 mM β-glycerophosphate, and 1 mM Na_3VO_4] containing 1% protease inhibitor (Sigma). These samples were then sonicated on ice followed by centrifugation at 15,000 × *g* for 10 min at 4°C to collect the supernatant. The protein concentration was determined using the bicinchoninic acid assay (BCA, Thermo Fisher Scientific, Waltham, MA, USA). The protein concentration of each sample was normalized before mixing with a half volume of SDS-PAGE loading buffer [6% SDS, 62.5 mM Tris-HCl (pH 6.8), 24% glycerol, 15% 2-ME, and 0.015% bromophenol blue] and then heated for 5 min at 95°C. The proteins were separated via SDS-PAGE and then electro-transferred onto PVDF membranes (Pall Corporation, Pensacola, FL, USA) at 2 mA/cm^2 for 1 hr. The membranes were blocked with 5% skim milk in TBS-T [20 mM Tris-HCl (pH 7.5), 150 mM NaCl, and 0.1% Tween 20] for 1 hr at room temperature, incubated with the indicated primary antibodies overnight at 4°C, and then reacted with HRP-linked secondary antibodies at room temperature for 1 hr. The immunoreactive proteins on the membranes were detected via enhanced chemiluminescence using Chemi-Lumi One L (Nacalai Tesque, Kyoto, Japan). The presented results are representative of three or more experiments. The band intensity was measured using ImageJ software (Wayne Rasband, National Institutes of Health, USA).

H_2O_2 detection

A431 cells seeded in 8-well chambers (Matsunami Glass Ind., Osaka, Japan) for quantitation or 96-well Nunclon delta black plates (Thermo Fisher Scientific) for quantification were pretreated with or without PEG-CAT (3000 U/mL) for 1 hr and then incubated for 20 min with 5 μM HYDROP, which is a specific probe for the detection of intracellular H_2O_2 (Abo *et al*., 2011). The cells were exposed to indicated compounds for 10 min, followed by washing twice with D-PBS. Fluorescence was observed using a confocal microscope (Nikon C2, Nikon Instech Co., Tokyo, Japan) or quantified using a microplate reader (Spectra Max M2, Molecular Devices, Tokyo, Japan) at excitation and emission wavelengths of 488 and 516 nm, respectively.

Cytotoxicity assay

After exposure to compounds in 96-well plates, A431 cells were treated with 5 mg/mL MTT solution (1/20, v/v)

for 20 min in a CO_2 incubator at 37°C. After removing the medium, DMSO (100 μL/well) was added, followed by incubation at room temperature for 30 min to dissolve formazan. The absorbance was measured at 540 nm using a spectrophotometer (iMark Microplate Absorbance Reader, Bio-Rad).

Immunoprecipitation of oxidized PTPs

A431 cells were exposed to 9,10-PQ or DDP for 10 min and then lysed using lysis buffer containing 10 mM IAA and 200 U/mL CAT. The protein concentration was determined using the BCA assay. The cell lysates (300 μg of protein) were denatured in 0.5% SDS in PBS (final volume of 200 μL) at 95°C for 10 min. The samples were then incubated with 30 μL of anti-mouse IgG conjugated magnetic beads (Dynabeads M-280 Sheep anti-mouse IgG, Novex, Life Technologies) and 1.5 μg of oxPTP Ab at 4°C overnight with gentle shaking. The beads were collected and washed four times with PBS. The protein complexes were eluted by adding 30 μL of 0.1 M glycine (pH 3.0), followed by UPLC-MS^E analysis. ProteinLynx global server browser version 2.3 software (Waters) was used to identify the protein.

Detection of Prx1 oxidation

Dimerization of peroxiredoxin 1 (Prx1) was detected according to the method described in the previous study (Cox *et al*., 2010) with a slight modification. A431 cells were exposed to 9,10-PQ or DDP, washed three times with cold D-PBS, lysed by lysis buffer containing 100 mM *N*-ethylmaleimide, 200 U/mL CAT, and 1% protease inhibitor. The samples were then incubated at −80°C overnight, followed by centrifugation at 15,000 × *g* for 10 min at 4°C to collect the supernatant. The cell lysates were subjected to non-reduced and reduced SDS-PAGE, followed by Western blotting using anti-Prx1 antibody (Ishii *et al*., 1995).

Data analysis

All data are presented as the mean ± SE from at least three independent experiments. Statistical significance was assessed using one- or two-way ANOVA, followed by a Dunnett multiple-comparison test using GraphPad Prism version 6.0 software (San Diego, CA, USA). $p < 0.05$ was considered significant.

RESULTS

Involvement of S-oxidation by 9,10-PQ–produced H_2O_2 in PTP1B inhibition

Recombinant hPTP1B was incubated with 9,10-PQ in the presence of DTT, which reduces 9,10-PQ to activate redox cycling (Kumagai *et al*., 2002), resulting in drastically decreased PTP activity in a concentration- and time-dependent manner (Fig. 1A–B). Next, we identified the modification site of hPTP1B by H_2O_2 derived from the redox cycling of 9,10-PQ. hPTP1B-SOH was labeled by dimedone because of its instability. As shown in Fig. 1C, the band intensities of dimedone-labeled hPTP1B-SOH and hPTP1B-SO_3H were significantly increased in a concentration-dependent manner. UPLC-MS^E revealed that hPTP1B significantly underwent *S*-oxidation corresponding to SOH, SO_2H, and SO_3H at Cys215, the active center of PTP1B (Fig. 1D–G, Tables S1–S6). By contrast, 9,10-PQ did not significantly oxidize other Cys residues such as Cys32, Cys92, and Cys121 under these conditions (Fig. S2).

To confirm the participation of H_2O_2 in the inhibition of PTP1B by 9,10-PQ, CAT was added to a reaction mixture of hPTP1B with 9,10-PQ. CAT prevented the inactivation of hPTP1B and the formation of P-SO_3H on its active site induced by 9,10-PQ in a concentration-dependent manner (Fig. 2A–B). In addition, there was no inhibition of hPTP1B activity during treatment with 9,10-PQ in the absence of DTT (Fig. S3), supporting the essential role of redox cycling in its inhibition. In fact, DDP, a 9,10-PQ derivative without redox capability, did not inactivate hPTP1B (Fig. 2C). These results indicate that the inactivation of PTP1B by 9,10-PQ is attributable to oxidation of its catalytic center Cys215 by H_2O_2 produced from the redox cycling of 9,10-PQ.

Suppression of cellular PTP activity in A431 cells by 9,10-PQ–produced ROS

The current consensus is that suppressing PTPs evokes the ligand-independent activation of EGFR signaling (Ostman *et al*., 2011; Denu and Tanner, 1998). Although the p*K*a of Cys is approximately 8.3 (Portillo-Ledesma *et al*., 2014), the catalytic Cys of PTPs has a thiol with an unusually low p*K*a of 4.7–5.6 that is present predominantly as a thiolate anion at physiological pH (Lohse *et al*., 1997; Zhang, 2003; Zhang and Dixon, 1993). The reactive thiol both catalyzes PTP activity as a nucleophile and renders PTPs highly susceptible to oxidation with concomitant inactivation (Denu and Tanner, 1998; Barford *et al*., 1998), suggesting that 9,10-PQ–derived ROS also oxidize and inactivate PTPs. Consistent with this finding, 9,10-PQ, but not DDP, significantly inhibited PTP activity in A431 cells and addition of DTT significantly recovered the inactivation by 9,10-PQ (Fig. 3A). Western blotting using oxPTP antibody, revealed the presence of at least two PTPs at molecular weights of approximately 50 and

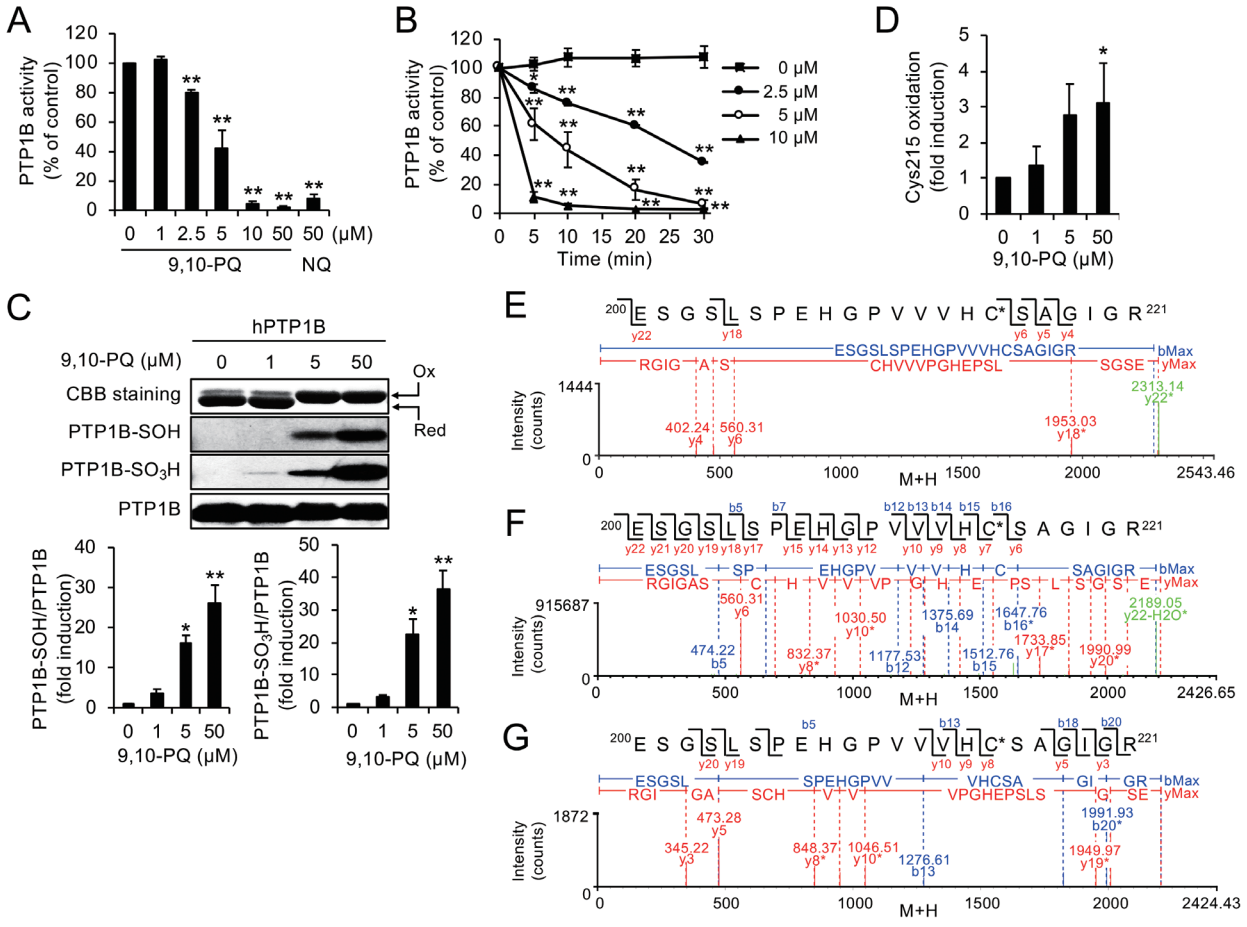

Fig. 1. Inactivation and *S*-oxidation of recombinant hPTP1B by 9,10-PQ. hPTP1B (13.5 μM) containing 1.25 mM DTT was incubated at 25°C with (A) 9,10-PQ or NQ for 10 min or (B) 9,10-PQ for 0–30 min in 50 mM Tris-HCl (pH 7.5)–0.1 mM EDTA. PTP1B activity was determined using a phosphatase assay. Each value is the mean ± SE of three determinations. *, $p < 0.05$; **, $p < 0.001$. (C) hPTP1B (13.5 μM) containing 1.25 mM DTT was incubated with 9,10-PQ at 25°C for 10 min, followed by treatment with 5 mM dimedone for 1 hr. The samples were analyzed by Western blotting using anti-2-thiodimedone–specific antibody, anti-oxPTP, anti-PTP1B antibody, and CBB staining. The band intensity was measured using ImageJ software. Each value is the mean ± SE of three independent experiments. *, $p < 0.01$; **, $p < 0.001$. (D) Site-specific oxidation was determined using UPLC-MS analysis by the ratio of peptides containing the oxidized forms of Cys to all peptides containing this site-specific Cys normalized to fold induction with the control group. Each value is the mean ± SE of three independent experiments. *, $p < 0.05$. Fragment sequences of oxidized hPTP1B determined by molecular mass analysis are shown in Tables S1, S2, and S3. (E–G) MS^E spectra of P-SOH labeled with dimedone (E), P-SO_2H (F), and P-SO_3H (G) containing the active site are shown. The corresponding MS^E data are shown in Tables S4, S5, and S6, respectively.

45 kDa, respectively, on SDS-PAGE that were oxidized at the active center during exposure to 9,10-PQ, but not DDP, in a concentration-dependent manner (Fig. 3B–C). UPLC-MS^E detected PTP1B, which is the ubiquitously expressed 50-kDa PTP in A431 cells and the prototypical member of the PTP family (Tonks, 2003; Lou *et al.*, 2008), with a coverage of 31% in the immunoprecipitated sample, indicating that the major band at 50 kDa was PTP1B (Fig. 3B–C, Table 1). The minor 45-kDa oxidized PTP might be T-cell PTP (45 or 48 kDa), which is also expressed in A431 cells (Baek *et al.*, 2018; Karisch *et al.*, 2011).

Activation of EGFR signaling by 9,10-PQ

PTPs dephosphorylate EGFR, leading to activation of downstream cascades such as MAPK/ERK signal. We therefore determined EGFR and ERK1/2 phosphorylation by 9,10-PQ in A431 cells. Exposure of A431 cells

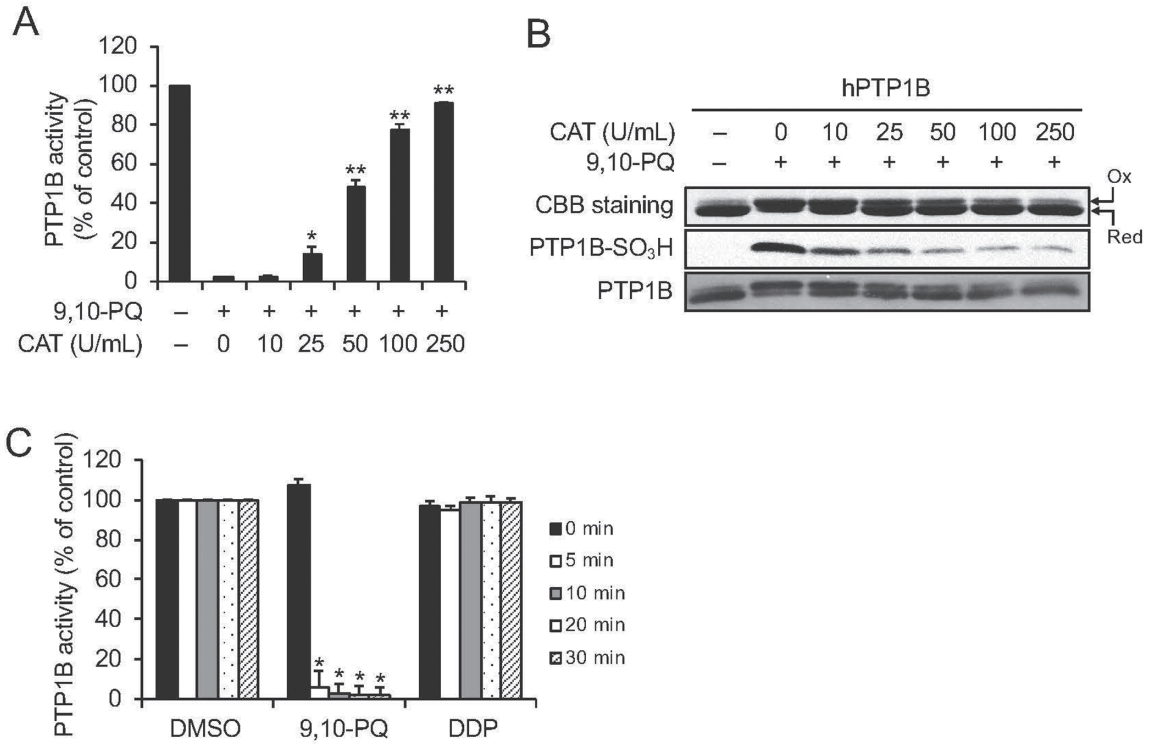

Fig. 2. H_2O_2-mediated inhibition of hPTP1B activity caused by 9,10-PQ. hPTP1B (13.5 μM) containing 1.25 mM DTT and 9,10-PQ (50 μM) was incubated with or without CAT for 30 min in 50 mM Tris-HCl (pH 7.5)−0.1 mM EDTA at 25°C. (A) PTP1B activity was determined using a phosphatase assay. Each value is the mean ± SE of three determinations. *, $p < 0.05$; **, $p < 0.001$. (B) The samples were subjected to Western blotting using oxPTP antibody, anti-PTP1B antibody, and CBB staining. (C) hPTP1B (13.5 μM) containing 1.25 mM DTT was incubated with 9,10-PQ (50 μM) or DDP (50 μM) for 30 min in 50 mM Tris-HCl (pH 7.5)−0.1 mM EDTA, and the phosphatase activity was determined. Each value is the mean ± SE of three determinations. *, $p < 0.001$.

to 9,10-PQ for 30 min resulted in EGFR and ERK1/2 phosphorylation in a concentration-dependent manner (Fig. 4A). 9,10-PQ–dependent EGFR and ERK1/2 activation at 1 μM reached a plateau at 5 min and then declined (Fig. 4B). Pretreatment of A431 cells with PD153035, an EGFR kinase inhibitor (Fry *et al*., 1994), prior to exposure to 9,10-PQ significantly diminished the phosphorylation of EGFR and ERK1/2 (Fig. 4C), indicating that the 9,10-PQ–dependent activation of ERK1/2 is mediated by EGFR phosphorylation.

Because ERK1/2 regulates cell proliferation and survival (Zhang and Liu, 2002), we speculated that the activation of EGFR-ERK1/2 signaling by 9,10-PQ at non-toxic concentrations might enhance cell proliferation against 9,10-PQ–mediated cell death at higher concentrations. As shown in Fig. 4D, 9,10-PQ significantly increased cell proliferation at concentrations of 0.5 μM or lower, whereas cell viability declined at higher concentrations. Pretreatment with the EGFR kinase inhibitor PD153035 significantly suppressed the increased cell viability detected during exposure to lower concentrations of 9,10-PQ and enhanced the cell death during exposure to 9,10-PQ (up to 3.75 μM). The LC_{50} in the presence of PD153035 (3.33 ± 0.18 μM) was lower than that in its absence (4.11 ± 0.2 μM), indicating that the activation of EGFR-ERK1/2 signaling mediated by 9,10-PQ mitigates 9,10-PQ–induced toxic effects.

Involvement of H_2O_2 produced from 9,10-PQ redox cycling in the activation of EGFR-ERK1/2 signaling

Exposure of A431 cells to 9,10-PQ, but not DDP, for 10 min enhanced intracellular H_2O_2 levels detected using HYDROP, which is a highly specific probe for intracellular H_2O_2 (Abo *et al*., 2011), in a concentration-dependent manner (Fig. 5A–B). To investigate whether H_2O_2 is involved in the 9,10-PQ–mediated activation of EGFR-ERK1/2 signaling, A431 cells were pretreated with the

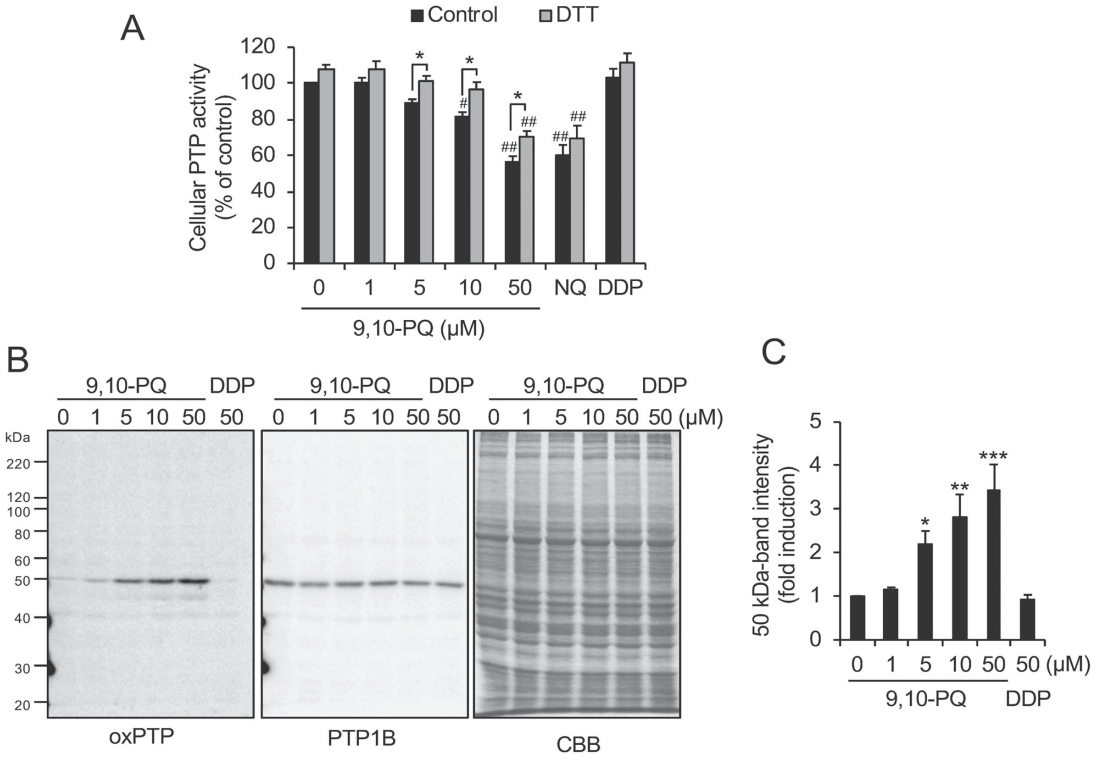

Fig. 3. Inhibition of cellular PTP activity via *S*-oxidation by 9,10-PQ. (A) A431 cells were exposed to 9,10-PQ (0–50 μM), NQ (50 μM), or DDP (50 μM) for 30 min. The cell lysate preparation was subjected to a phosphatase assay in the presence or absence of DTT (10 mM). Data are presented as the mean ± SE of four independent experiments and expressed as a percentage of the initial activity. *, $p < 0.05$. #, $p < 0.05$; ##, $p < 0.01$ *vs*. 0 μM. (B) A431 cells were exposed to 9,10-PQ (0–50 μM) or DDP (50 μM) for 10 min. The cell lysates were analyzed by Western blotting using anti-oxPTP antibody, anti-PTP1B antibody, and CBB staining. (C) The band intensity of Western blotting results at approximately 50 kDa was measured using ImageJ software. Each value is the mean ± SE of three independent determinations. *, $p < 0.05$; **, $p < 0.01$; ***, $p < 0.001$.

Table 1. Fragment sequences of PTP1B determined by UPLC-MS^E.

Peak No.	Observed MS (Da)	Calculated MS (Da)	Error (Da)	Position	Retention time (min)	Sequence
1	1366.67	1366.68	-0.0048	13−24	52.14	(K)SGSWAAIYQDIR(H)
2	1197.64	1197.65	-0.0079	269−279	54.38	(R)FSYLAVIEGAK(F)
3	1772.89	1772.88	0.0039	59−73	42.32	(K)LHQEDNDYINASLIK(M)
4	2664.40	2664.39	0.009	293−315	36.59	(K)ELSHEDLEPPPEHIPPPPRPPKR(I)
5	1378.65	1378.65	-0.0046	46−56	31.74	(R)YRDVSPFDHSR(I)
6	2508.28	2508.29	-0.0091	293−314	38.48	(K)ELSHEDLEPPPEHIPPPPRPPK(R)
7	1574.80	1574.80	0.0005	157−169	44.59	(R)QLELENLTTQETR(E)
8	2232.07	2232.08	-0.0099	200−221	35.09	(R)ESGSLSPEHGPVVVHCSAGIGR(S)
9	3339.77	3339.65	0.1224	170−197	56.13	(R)EILHFHYTTWPDFGVPESPASFLNFLFK(V)

A431 cells were exposed to 9,10-PQ (50 μM) for 10 min. The cell lysate was collected and immunoprecipitated by using anti-oxPTP antibody as described in the method section. The oxidized PTPs were eluted using 0.1 M glycine (pH 3) and then subjected to UPLC-MS^E analysis. ProteinLynx global server browser version 2.3 software was used to identify the protein.

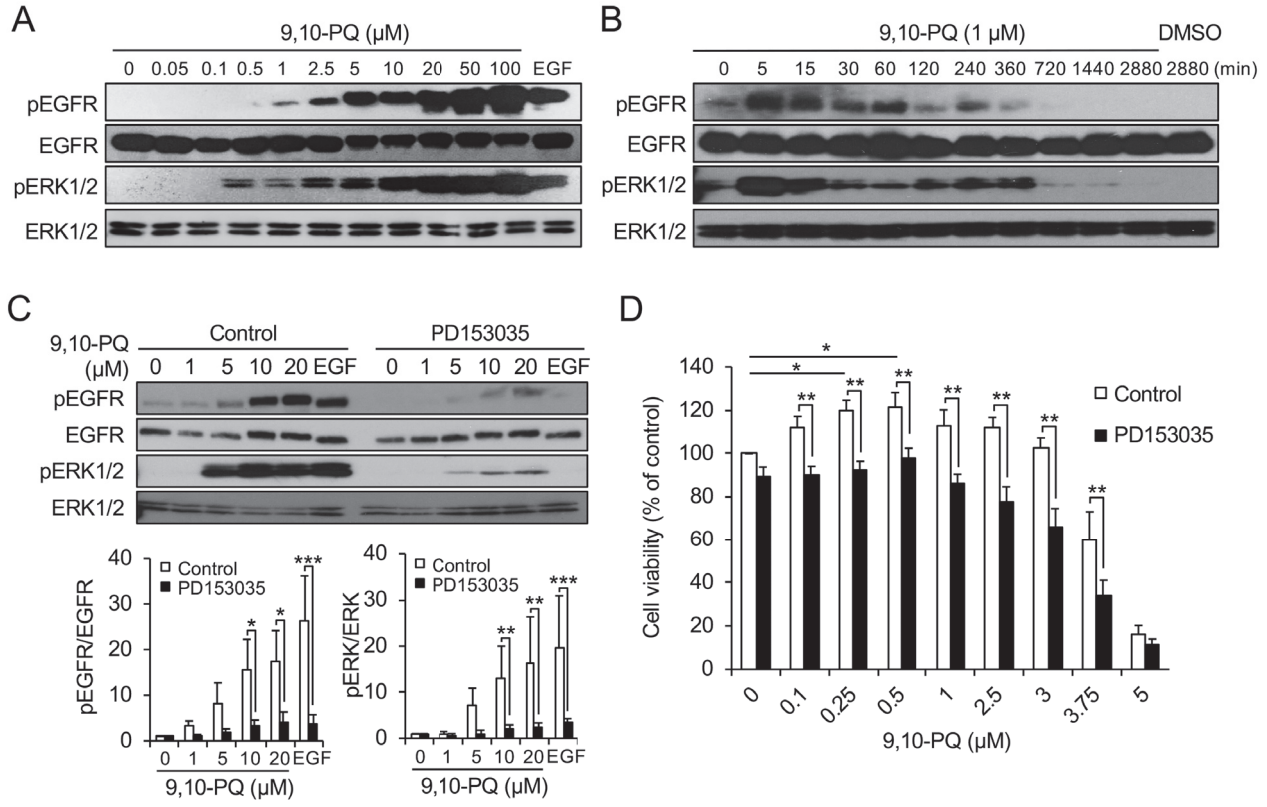

Fig. 4. Activation of EGFR signaling and the effect of EGFR inhibition on cell viability during exposure to 9,10-PQ. A431 cells were exposed to (A) 9,10-PQ (0–100 μM) or EGF (5 ng/mL) for 30 min, (B) 9,10-PQ (1 μM) or DMSO for 0–48 hr, or (C) 9,10-PQ (0–20 μM) or EGF (5 ng/mL) for 30 min after pretreatment with or without PD153035 (1 μM) for 2 hr. The cell lysates were subjected to Western blotting. The band intensity of the Western blotting results was measured using ImageJ software. Each value is the mean ± SE of three independent experiments. *, $p < 0.05$; **, $p < 0.01$; ***, $p < 0.001$. (D) A431 cells were pretreated with or without PD153035 (1 μM) for 2 hr and then exposed to 9,10-PQ for 24 hr. Cell viability was examined using the MTT assay. LC_{50} was determined using Prism software. Each value is the mean ± SE of three independent experiments. *, $p < 0.05$; **, $p < 0.01$.

H_2O_2 scavenger PEG-CAT for 1 hr before treatment with 9,10-PQ. As shown in Fig. 5A–B, PEG-CAT (3000 U/mL) significantly scavenged the 9,10-PQ-produced H_2O_2. Under these conditions, PEG-CAT abolished the activation of EGFR-ERK1/2 signaling and decreased cytotoxicity during exposure to 9,10-PQ (Fig. 5C–D). In addition, unlike 9,10-PQ, DDP, which lacks redox activity, did not affect the EGFR-ERK1/2 cascade or cell viability (Fig. 5E–F). These observations suggest that 9,10-PQ interacts with cellular electron donors in A431 cells, leading to the generation of H_2O_2, which can substantially activate EGFR-ERK1/2 signaling. Besides oxidation of PTP1B, we also evaluated whether or not Prx1, which easily undergoes oxidation (Rhee and Kil, 2017), could be dimerized during exposure of the cells to 9,10-PQ. As shown in Fig. 6, dimerized Prx1 based on its oxidized form was significantly increased by 9,10-PQ, but not DDP, in a concentration-dependent manner, indicating that 9,10-PQ–derived H_2O_2 also caused the oxidative status of Prx1 in the cells.

Simultaneous treatment with the iron chelator 1,10-phenanthroline or ·OH scavenger thiourea (25 mM) also significantly suppressed cell death caused by 9,10-PQ (data not shown). However, 1,10-phenanthroline and thiourea did not diminish the 9,10-PQ–mediated phosphorylation of EGFR and ERK1/2 under these conditions (Fig. 7). These results suggest that the generation of ·OH and iron did not contribute to the activation of EGFR-ERK1/2 signaling by 9,10-PQ.

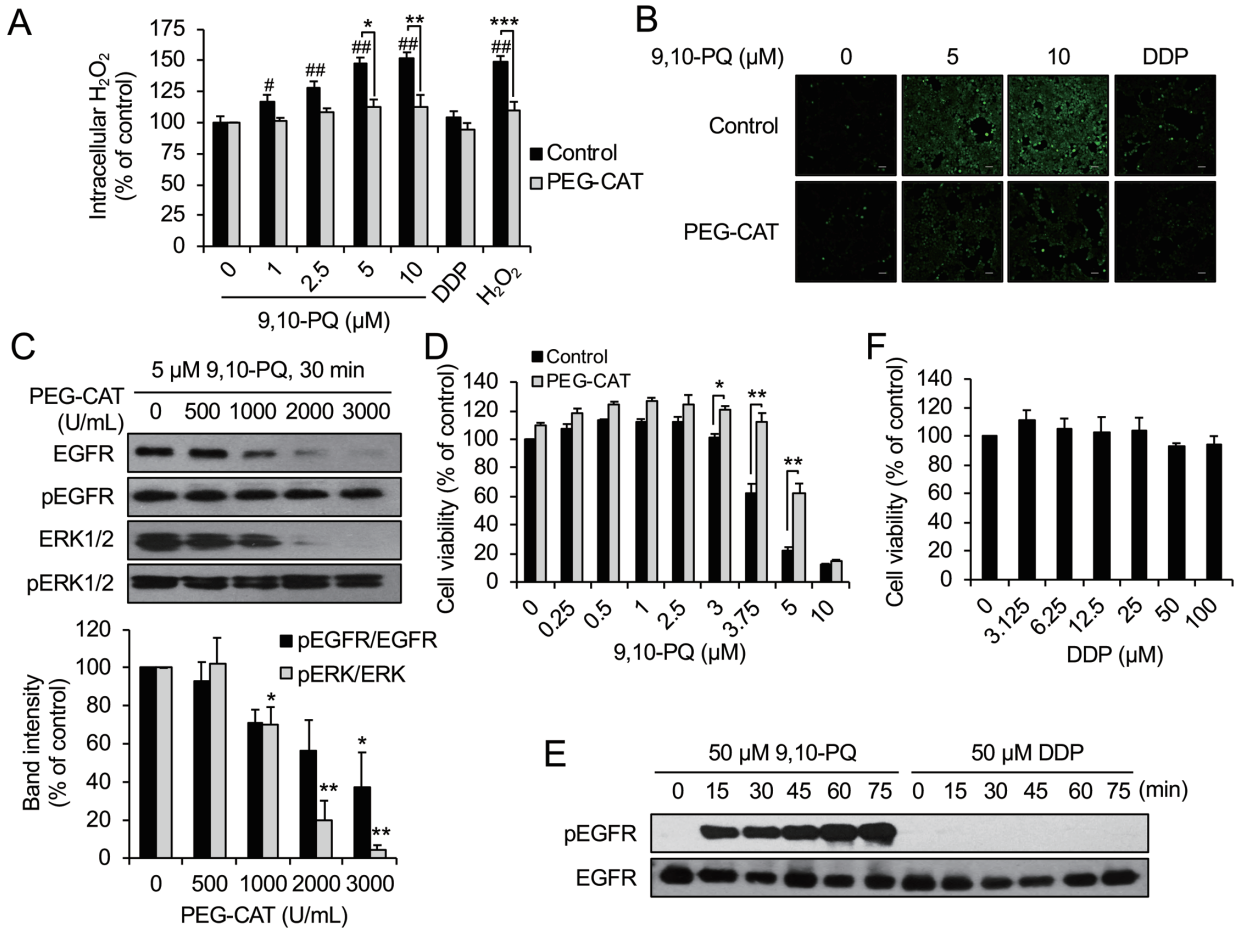

Fig. 5. Involvement of H_2O_2 generated by 9,10-PQ in the activation of EGFR signaling. (A, B) A431 cells were pretreated with or without PEG-CAT (3000 U/mL) for 1 hr and incubated with 5 μM HYDROP for 20 min. The cells were then exposed to (A) 9,10-PQ, DDP (50 μM), or H_2O_2 (500 μM); (B) 9,10-PQ or DDP (50 μM) for 10 min. The fluorescence intensity was determined using a fluorescence plate reader (A) or a confocal microscope (scale bar: 50 μm) (B). Data are presented in (A) as the mean ± SE of four independent experiments and expressed as a percentage of the initial activity. *, $p < 0.05$; **, $p < 0.01$; ***, $p < 0.001$. #, $p < 0.05$; ##, $p < 0.01$ *vs*. 0 μM. (C) The cells were pretreated with PEG-CAT for 1 hr and exposed to 9,10-PQ for 30 min. The cell lysates were subjected to Western blotting, and the band intensity was quantified using ImageJ software. Data are presented as the mean ± SE of three independent experiments and expressed as a percentage of the initial activity. *, $p < 0.05$; **, $p < 0.01$. (D) The cells were pretreated with 3000 U/mL PEG-CAT for 1 hr, followed by exposure to 9,10-PQ for 24 hr. Cell viability was determined using the MTT assay. Data are presented as the mean ± SE of three independent experiments and expressed as a percentage of the initial activity. *, $p < 0.01$; **, $p < 0.001$. (E) The cells were exposed to 9,10-PQ or DDP for 0–75 min and then analyzed via Western blotting. (F) The cells were exposed to DDP for 24 hr. Cell viability was examined using the MTT assay. Each value is the mean ± SE of three independent experiments.

DISCUSSION

The present study identified 9,10-PQ that can activate PTP-EGFR signaling through *S*-oxidation of PTPs such as PTP1B by H_2O_2 *via* redox cycling. Binding of EGF to its receptor triggers the production of $O_2^{\bullet-}$ through the enzymatic activity of the NADPH oxidase family, followed by the rapid conversion of $O_2^{\bullet-}$ to H_2O_2 through dispropor-tionation (Nauseef, 2014; Lambeth, 2004). Endogenous H_2O_2 oxidizes PTP1B to its P-SOH, leading to activation of the EGFR signal cascade (Bae *et al*., 1997; Lee *et al*., 1998). We speculated that ROS generated by exogenous chemicals can mimic endogenous ROS and thus activate such redox signaling pathways. Because 9,10-PQ is a good electron acceptor that can produce excessive levels of ROS via redox cycling (Kumagai *et al*., 2002; Taguchi

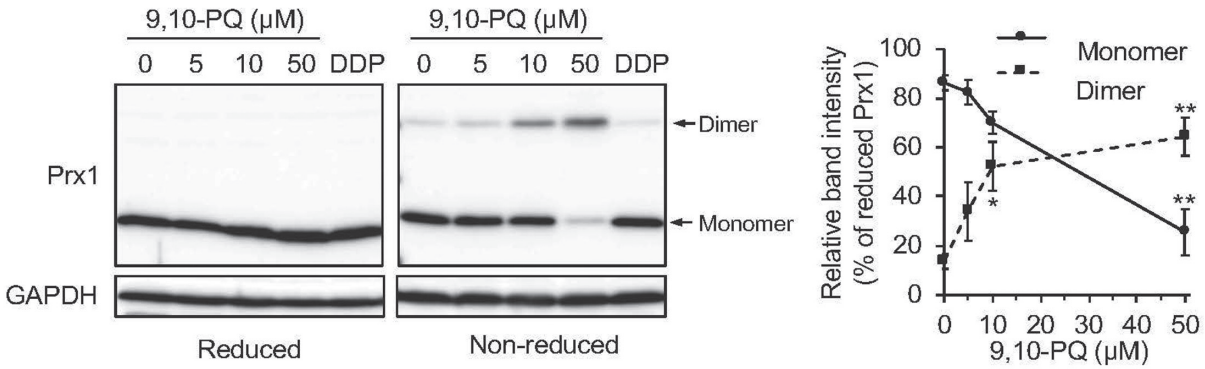

Fig. 6. Oxidation of cellular Prx1 caused by 9,10-PQ. A431 cells were exposed to 9,10-PQ (0–50 μM) or DDP (50 μM) for 45 min. The cells were lysed into lysis buffer containing 100 mM *N*-ethylmaleimide, 200 U/mL CAT, and 1% protease inhibitor and then subjected to non-reduced and reduced SDS-PAGE (A). The band intensity was quantified using ImageJ software (B). Data are presented as the mean ± SE of three independent experiments. *, $p < 0.01$; **, $p < 0.001$.

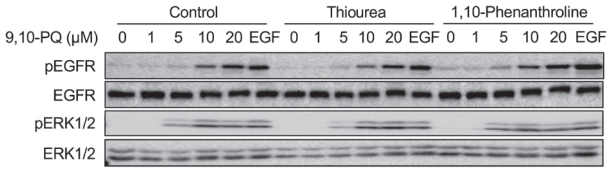

Fig. 7. Effect of an iron chelator and a hydroxyl radical scavenger on the 9,10-PQ–mediated activation of EGFR-ERK1/2 signaling. A431 cells were pretreated with thiourea (100 mM) or 1,10-phenanthroline (10 μM) for 30 min, followed by exposure to 9,10-PQ or EGF (5 ng/mL) for 30 min. The cell lysates were subjected to Western blotting. The data are representative of three independent determinations.

et al., 2007, 2008), 9,10-PQ–produced H_2O_2 is postulated to activate the aforementioned signaling pathways.

H_2O_2 at lower concentrations causes the *S*-oxidation of sensor proteins to form P-SOH, which can be reduced to its original form by cellular reductants such as Trx and glutathione, resulting in the transient activation of cellular redox signaling (Poole *et al*., 2004). By contrast, H_2O_2 at higher concentrations further oxidize P-SOH to P-SO_2H and ultimately to P-SO_3H. Although recent evidence suggests that P-SO_2H (e.g., Prxs) can be reduced by enzymes such as sulfiredoxin (Biteau *et al*., 2003; Jeong *et al*., 2006; Akter *et al*., 2018), no enzymes that can reduce P-SO_3H back to P-SH have been described. The catalytic domain of PTP1B has a highly nucleophilic Cys residue (Cys215) with a lower p*K*a (approximately 5.4), making it a favorable target for oxidation (Lohse *et al*., 1997). Whereas endogenous H_2O_2 oxidizes P-SH on Cys215 to yield the reversible oxidized form P-SOH (Lee *et al*., 1998), the PTP inhibitor pervanadate inactivates PTP1B via the *S*-oxidation of Cys215 to form P-SO_3H, an irreversible form (Huyer *et al*., 1997). Regarding 9,10-PQ, however, this exogenous quinone oxidized Cys215 to form P-SOH, P-SO_2H, and P-SO_3H (Fig. 1), suggesting that the active site of Cys215 readily undergoes *S*-oxidation mediated by H_2O_2. Under our experimental conditions, we observed little oxidation at Cys32, Cys92, or Cys121 (Fig. S2). This suggests that the H_2O_2-mediated redox cycling of 9,10-PQ has a key role in oxidizing the active site of PTP1B, resulting in inhibition of its catalytic activity. In A431 cells, our immunoprecipitation assay using anti-oxPTP antibody revealed that PTP1B was oxidized during 9,10-PQ exposure. Whereas the catalytic Cys of PTPs has a low p*K*a thiol (ranging from 4.7 to 5.6), which renders PTPs highly susceptible to oxidation with concomitant inactivation, PTP1B is a target of 9,10-PQ–derived H_2O_2 as reported previously (Lee *et al*., 1998; Dagnell *et al*., 2013, 2019). Recently, Dagnell *et al.* (2019) found that peroxymonocarbonate, which is generated by the reaction of H_2O_2 with bicarbonate, is an obligate factor for EGF-dependent PTP1B oxidation *in vitro*, including in A431 cells. We therefore speculate that H_2O_2 generated from the redox cycling of 9,10-PQ might, at least in part, react with bicarbonate hydrated from CO_2 to yield peroxymonocarbonate, leading to the oxidation of PTP1B. Cenas *et al*. (2004) reported that 9,10-PQ is a substrate for NADPH-dependent TrxR, suggesting that such an enzyme may contribute to a redox cycling of 9,10-PQ in the cells. While 9,10-PQ consumed NADPH in the presence of TrxR *in vitro* (Fig. S4), 9,10-PQ did not affect TrxR activity in A431 cell lysate when insulin was

used as the substrate (Fig. S5). It seems likely that 9,10-PQ is not efficient substrate for the enzyme, resulting in promotion of redox cycling of 9,10-PQ in the cells. Since oxidized PTP1B is found to be a substrate for TrxR (Dagnell *et al*., 2017), it should be noted that 9,10-PQ could affect reactivation of PTP1B mediated by TrxR.

Although the current consensus is that the suppression of PTPs evokes the ligand-independent activation of EGFR signaling (Ostman *et al*., 2011; Denu and Tanner, 1998), we speculated that 9,10-PQ, but not its analog DDP lacking redox capability, could inhibit PTP activity in A431 cells, leading to EGFR phosphorylation. As expected, exposure of A431 cells to 9,10-PQ resulted in phosphorylation of EGFR and its downstream kinase ERK1/2 (Fig. 4A–B). ERK1/2 phosphorylation was suppressed by an EGFR inhibitor, indicating that the 9,10-PQ–mediated phosphorylation of ERK1/2 was dependent on EGFR activation under the experimental conditions (Fig. 4C). Interestingly, the increase in cell viability induced by lower concentrations of 9,10-PQ (0.1–0.5 μM) was diminished by an EGFR inhibitor (Fig. 4D), indicating that 9,10-PQ enhances cell proliferation through the activation of EGFR signaling; however, higher concentrations of the electron acceptor might generate high levels of ROS that exceed the capacity of the cellular defense system, leading to cell death. Pretreatment with the H_2O_2 scavenger PEG-CAT significantly diminished 9,10-PQ–dependent intracellular H_2O_2 accumulation and EGFR and ERK1/2 activation (Fig. 5A–C). In addition, DDP did not exert any cytotoxic effects or activate EGFR and ERK1/2 in A431 cells (Fig. 5E–F). These results indicated that 9,10-PQ activates EGFR-ERK1/2 signaling through the oxidative inactivation of PTPs such as PTP1B. Recently, Paulsen *et al.* (2011) observed that sulfenylation of a critical Cys residue located within the intracellular kinase domain of EGFR (Cys797) by endogenous H_2O_2, as induced by NADPH oxidase activation, enhanced its tyrosine kinase activity. It should be noted that 9,10-PQ may also affect the activation of EGFR coupled to oxidative modification of this protein kinase.

H_2O_2 can react with free ferrous (or cuprous) ions to yield ferric (or cupric) ions, HO^-, and $^{\bullet}OH$, which are among the strongest oxidants (Winterbourn, 1995). $O_2^{\bullet-}$ interacts with ferritin, which is a major source of iron in cells, to release ferric, which is subsequently oxidized to ferrous by $O_2^{\bullet-}$ (Biemond *et al*., 1984). The $^{\bullet}OH$ scavenger thiourea and ferric chelator 1,10-phenanthroline had little effect on the 9,10-PQ–mediated activation of EGFR and ERK (Fig. 7), strongly indicating H_2O_2 rather than $^{\bullet}OH$ contributes to signal activation by 9,10-PQ. However, 1,10-phenanthroline and thiourea protected the cells against 9,10-PQ–mediated cell death (data not shown), indicating that 9,10-PQ–mediated cell damage is, at least partially, attributable to $^{\bullet}OH$ derived from excess H_2O_2 generated by redox cycling of the electron acceptor. Supporting this finding, we previously reported that 9,10-PQ induces $^{\bullet}OH$ formation in the presence of iron or ferritin *in vitro* and that 1,10-phenanthroline inhibits 9,10-PQ-mediated toxicity, protein oxidation, and DNA fragmentation in A549 cells (Sugimoto *et al*., 2005). Akhiani *et al.* reported that ROS activated ERK1/2 and subsequently PARP-1, leading to a form of programmed cell death, parthanatos, in human lymphocytes (Akhiani *et al*., 2014). Whereas 9,10-PQ causes apoptosis (Sugimoto *et al*., 2005; Taguchi *et al*., 2007), the quinone might also induce parthanatos through ROS generation. Such a possibility is being studied in our laboratory.

The present study found that a model electron acceptor 9,10-PQ activated EGFR-ERK1/2 signaling in A431 cells, presumably through *S*-oxidation of the active site of PTP1B by H_2O_2 generated via redox cycling (Fig. 8). Although there is little doubt that 9,10-PQ exposure at high concentrations causes oxidative damage and cell death, activation of EGFR signaling during exposure to 9,10-PQ at lower concentrations may be involved, at least in part, in cell survival.

ACKNOWLEDGMENT

This work was supported in part by a Grant-in-Aid for Scientific Research on Innovative Areas “Oxygen Biology: a new criterion for integrated understanding of life” (#17H05519 to Y.K.) and a Grant-in-Aid (#17K15489 to Y.A.) for Scientific Research from the Ministry of Education, Culture, Sports, Science and Technology of Japan. MarvinSketch was used to draw Fig. 8, Product version 17.21.0, ChemAxon (https://www.chemaxon.com). We thank Joe Barber Jr., PhD, from Edanz Group (www.edanzediting.com/ac) for editing a draft of this manuscript.

Conflict of interest---- The authors declare that there is no conflict of interest.

REFERENCES

Abiko, Y., Nakai, Y., Luong, N.C., Bianco, C.L., Fukuto, J.M. and Kumagai, Y. (2019): Interaction of quinone-related electron acceptors with hydropersulfide Na_2S_2: evidence for one-electron reduction reaction. Chem. Res. Toxicol., **32**, 551-556.

Abo, M., Urano, Y., Hanaoka, K., Terai, T., Komatsu, T. and Nagano, T. (2011): Development of a highly sensitive fluorescence probe for hydrogen peroxide. J. Am. Chem. Soc., **133**, 10629-10637.

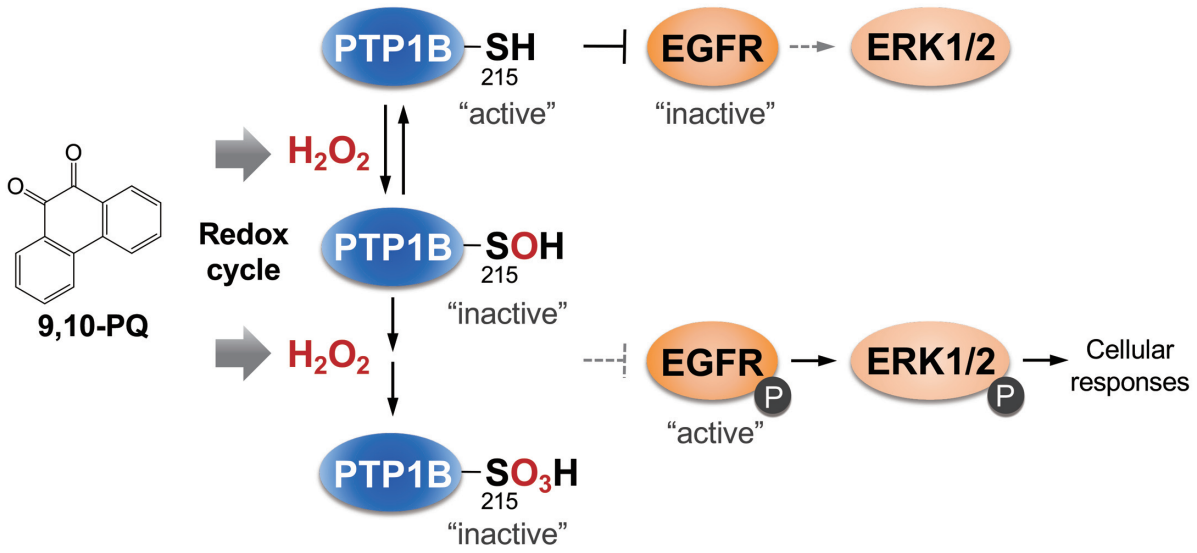

Fig. 8. Activation of PTP1B-EGFR signaling through the *S*-oxidation of PTPs by 9,10-PQ–generated H_2O_2 via redox cycling. ERK1/2, extracellular signal-regulated kinase 1/2; SOH, sulfenic acid; SO_3H, sulfonic acid.

Akhiani, A.A., Werlenius, O., Aurelius, J., Movitz, C., Martner, A., Hellstrand, K. and Thorén, F.B. (2014): Role of the ERK pathway for oxidant-induced parthanatos in human lymphocytes. PLoS One, **9**, e89646.

Akter, S., Fu, L., Jung, Y., Conte, M.L., Lawson, J.R., Lowther, W.T., Sun, R., Liu, K., Yang, J. and Carroll, K.S. (2018): Chemical proteomics reveals new targets of cysteine sulfinic acid reductase. Nat. Chem. Biol., **14**, 995-1004.

Bae, Y.S., Kang, S.W., Seo, M.S., Baines, I.C., Tekle, E., Chock, P.B. and Rhee, S.G. (1997): Epidermal growth factor (EGF)-induced generation of hydrogen peroxide. Role in EGF receptor-mediated tyrosine phosphorylation. J. Biol. Chem., **272**, 217-221.

Baek, M., Kim, M., Lim, J.S., Morales, L.D., Hernandez, J., Mummidi, S., Williams-Blangero, S., Jang, I.S., Tsin, A.T. and Kim, D.J. (2018): Epidermal-specific deletion of TC-PTP promotes UVB-induced epidermal cell survival through the regulation of Flk-1/JNK signaling. Cell Death Dis., **9**, 730.

Barford, D., Das, A.K. and Egloff, M.P. (1998): The structure and mechanism of protein phosphatases: insights into catalysis and regulation. Annu. Rev. Biophys. Biomol. Struct., **27**, 133-164.

Barrett, W.C., DeGnore, J.P., König, S., Fales, H.M., Keng, Y.F., Zhang, Z.Y., Yim, M.B. and Chock, P.B. (1999): Regulation of PTP1B via glutathionylation of the active site cysteine 215. Biochemistry, **38**, 6699-6705.

Bhattacharya, S., Labutti, J.N., Seiner, D.R. and Gates, K.S. (2008): Oxidative inactivation of protein tyrosine phosphatase 1B by organic hydroperoxides. Bioorg. Med. Chem. Lett., **18**, 5856-5859.

Biemond, P., van Eijk, H.G., Swaak, A.J. and Koster, J.F. (1984): Iron mobilization from ferritin by superoxide derived from stimulated polymorphonuclear leukocytes. Possible mechanism in inflammation diseases. J. Clin. Invest., **73**, 1576-1579.

Biteau, B., Labarre, J. and Toledano, M.B. (2003): ATP-dependent reduction of cysteine-sulphinic acid by S. cerevisiae sulphiredoxin. Nature, **425**, 980-984.

Bradford, M.M. (1976): A rapid and sensitive method for the quantitation of microgram quantities of protein utilizing the principle of protein-dye binding. Anal. Biochem., **72**, 248-254.

Cenas, N., Nivinskas, H., Anusevicius, Z., Sarlauskas, J., Lederer, F. and Arnér, E.S. (2004): Interactions of quinones with thioredoxin reductase: a challenge to the antioxidant role of the mammalian selenoprotein. J. Biol. Chem., **279**, 2583-2592.

Cho, A.K., Di Stefano, E., You, Y., Rodriguez, C.E., Schmitz, D.A., Kumagai, Y. Miguel, A.H., Eiguren-Fernandez, A., Kobayashi, T., Avol, E. and Froines, J.R. (2004): Determination of four quinones in diesel exhaust particles, SRM 1649a, and atmospheric PM2.5 special issue of aerosol science and technology on findings from the fine particulate matter supersites program. Aerosol Sci. Technol., **38**, 68-81.

Chung, M.Y., Lazaro, R.A., Lim, D., Jackson, J., Lyon, J., Rendulic, D. and Hasson, A.S. (2006): Aerosol-borne quinones and reactive oxygen species generation by particulate matter extracts. Environ. Sci. Technol., **40**, 4880-4886.

Cohen, P., Klumpp, S. and Schelling, D.L. (1989): An improved procedure for identifying and quantitating protein phosphatases in mammalian tissues. FEBS Lett., **250**, 596-600.

Cox, A.G., Winterbourn, C.C. and Hampton, M.B. (2010): Measuring the redox state of cellular peroxiredoxins by immunoblotting. Methods Enzymol., **474**, 51-66.

Dagnell, M., Cheng, Q., Rizvi, S.H., Pace, P.E., Boivin, B., Winterbourn, C.C. and Arnér, E.S. (2019): Bicarbonate is essential for protein-tyrosine phosphatase 1B (PTP1B) oxidation and cellular signaling through EGF-triggered phosphorylation cascades. J. Biol. Chem., **294**, 12330-12338.

Dagnell, M., Frijhoff, J., Pader, I., Augsten, M., Boivin, B., Xu, J., Mandal, P.K., Tonks, N.K., Hellberg, C., Conrad, M., Arnér, E.S. and Östman, A. (2013): Selective activation of oxidized PTP1B by the thioredoxin system modulates PDGF-β receptor tyrosine kinase signaling. Proc. Natl. Acad. Sci. USA, **110**, 13398-13403.

Dagnell, M., Pace, P.E., Cheng, Q., Frijhoff, J., Östman, A., Arnér, E.S., Hampton, M.B. and Winterbourn, C.C. (2017): Thiore-

doxin reductase 1 and NADPH directly protect protein tyrosine phosphatase 1B from inactivation during H_2O_2 exposure. J. Biol. Chem., **292**, 14371-14380.

Denu, J.M. and Tanner, K.G. (1998): Specific and reversible inactivation of protein tyrosine phosphatases by hydrogen peroxide: evidence for a sulfenic acid intermediate and implications for redox regulation. Biochemistry, **37**, 5633-5642.

Dickinson, B.C. and Chang, C.J. (2011): Chemistry and biology of reactive oxygen species in signaling or stress responses. Nat. Chem. Biol., **7**, 504-511.

Fry, D.W., Kraker, A.J., McMichael, A., Ambroso, L.A., Nelson, J.M., Leopold, W.R., Connors, R.W. and Bridges, A.J. (1994): A specific inhibitor of the epidermal growth factor receptor tyrosine kinase. Science, **265**, 1093-1095.

Gamou, S., Kim, Y.S. and Shimizu, N. (1984): Different responses to EGF in two human carcinoma cell lines, A431 and UCVA-1, possessing high numbers of EGF receptors. Mol. Cell. Endocrinol., **37**, 205-213.

Huyer, G., Liu, S., Kelly, J., Moffat, J., Payette, P., Kennedy, B., Tsaprailis, G., Gresser, M.J. and Ramachandran, C. (1997): Mechanism of inhibition of protein-tyrosine phosphatases by vanadate and pervanadate. J. Biol. Chem., **272**, 843-851.

Ishii, T., Kawane, T., Taketani, S. and Bannai, S. (1995): Inhibition of the thiol-specific antioxidant activity of rat liver MSP23 protein by hemin. Biochem. Biophys. Res. Commun., **216**, 970-975.

Iwamoto, N., Sumi, D., Ishii, T., Uchida, K., Cho, A.K., Froines, J.R. and Kumagai, Y. (2007): Chemical knockdown of protein-tyrosine phosphatase 1B by 1,2-naphthoquinone through covalent modification causes persistent transactivation of epidermal growth factor receptor. J. Biol. Chem., **282**, 33396-33404.

Jeong, W., Park, S.J., Chang, T.S., Lee, D.Y. and Rhee, S.G. (2006): Molecular mechanism of the reduction of cysteine sulfinic acid of peroxiredoxin to cysteine by mammalian sulfiredoxin. J. Biol. Chem., **281**, 14400-14407.

Jones, D.P. (2008): Radical-free biology of oxidative stress. Am. J. Physiol. Cell Physiol., **295**, C849-C868.

Karisch, R., Fernandez, M., Taylor, P., Virtanen, C., St-Germain, J.R., Jin, L.L., Harris, I.S., Mori, J., Mak, T.W., Senis, Y.A., Östman, A., Moran, M.F. and Neel, B.G. (2011): Global proteomic assessment of the classical protein-tyrosine phosphatome and "Redoxome". Cell, **146**, 826-840.

Kumagai, Y., Koide, S., Taguchi, K., Endo, A., Nakai, Y., Yoshikawa, T. and Shimojo, N. (2002): Oxidation of proximal protein sulfhydryls by phenanthraquinone, a component of diesel exhaust particles. Chem. Res. Toxicol., **15**, 483-489.

Lambeth, J.D. (2004): NOX enzymes and the biology of reactive oxygen. Nat. Rev. Immunol., **4**, 181-189.

Lee, S.R., Kwon, K.S., Kim, S.R. and Rhee, S.G. (1998): Reversible inactivation of protein-tyrosine phosphatase 1B in A431 cells stimulated with epidermal growth factor. J. Biol. Chem., **273**, 15366-15372.

Lohse, D.L., Denu, J.M., Santoro, N. and Dixon, J.E. (1997): Roles of aspartic acid-181 and serine-222 in intermediate formation and hydrolysis of the mammalian protein-tyrosine-phosphatase PTP1. Biochemistry, **36**, 4568-4575.

Lou, Y.W., Chen, Y.Y., Hsu, S.F., Chen, R.K., Lee, C.L., Khoo, K.H., Tonks, N.K. and Meng, T.C. (2008): Redox regulation of the protein tyrosine phosphatase PTP1B in cancer cells. FEBS J., **275**, 69-88.

Marnett, L.J., Riggins, J.N. and West, J.D. (2003): Endogenous generation of reactive oxidants and electrophiles and their reactions with DNA and protein. J. Clin. Invest., **111**, 583-593.

Nauseef, W.M. (2014): Detection of superoxide anion and hydrogen peroxide production by cellular NADPH oxidases. Biochim. Biophys. Acta, **1840**, 757-767.

Ostman, A., Frijhoff, J., Sandin, A. and Böhmer, F.D. (2011): Regulation of protein tyrosine phosphatases by reversible oxidation. J. Biochem., **150**, 345-356.

Paulsen, C.E., Truong, T.H., Garcia, F.J., Homann, A., Gupta, V., Leonard, S.E. and Carroll, K.S. (2011): Peroxide-dependent sulfenylation of the EGFR catalytic site enhances kinase activity. Nat. Chem. Biol., **8**, 57-64.

Persson, C., Kappert, K., Engström, U., Ostman, A. and Sjöblom, T. (2005): An antibody-based method for monitoring *in vivo* oxidation of protein tyrosine phosphatases. Methods, **35**, 37-43.

Persson, C., Sjöblom, T., Groen, A., Kappert, K., Engström, U., Hellman, U., Heldin, C.H., den Hertog, J. and Ostman, A. (2004): Preferential oxidation of the second phosphatase domain of receptor-like PTP-alpha revealed by an antibody against oxidized protein tyrosine phosphatases. Proc. Natl. Acad. Sci. USA, **101**, 1886-1891.

Poole, L.B., Karplus, P.A. and Claiborne, A. (2004): Protein sulfenic acids in redox signaling. Annu. Rev. Pharmacol. Toxicol., **44**, 325-347.

Portillo-Ledesma, S., Sardi, F., Manta, B., Tourn, M.V., Clippe, A., Knoops, B., Alvarez, B., Coitiño, E.L. and Ferrer-Sueta, G. (2014): Deconstructing the catalytic efficiency of peroxiredoxin-5 peroxidatic cysteine. Biochemistry, **53**, 6113-6125.

Rhee, S.G. and Kil, I.S. (2017): Multiple Functions and Regulation of Mammalian Peroxiredoxins. Annu. Rev. Biochem., **86**, 749-775.

Rodriguez, C.E., Fukuto, J.M., Taguchi, K., Froines, J. and Cho, A.K. (2005): The interactions of 9,10-phenanthrenequinone with glyceraldehyde-3-phosphate dehydrogenase (GAPDH), a potential site for toxic actions. Chem. Biol. Interact., **155**, 97-110.

Rodriguez, C.E., Shinyashiki, M., Froines, J., Yu, R.C., Fukuto, J.M. and Cho, A.K. (2004): An examination of quinone toxicity using the yeast Saccharomyces cerevisiae model system. Toxicology, **201**, 185-196.

Rudolph, T.K. and Freeman, B.A. (2009): Transduction of redox signaling by electrophile-protein reactions. Sci. Signal., **2**, re7.

Sakanyan, V., Hulin, P., Alves de Sousa, R., Silva, V.A., Hambardzumyan, A., Nedellec, S., Tomasoni, C., Logé, C., Pineau, C., Roussakis, C., Fleury, F. and Artaud, I. (2016): Activation of EGFR by small compounds through coupling the generation of hydrogen peroxide to stable dimerization of Cu/Zn SOD1. Sci. Rep., **6**, 21088.

Seth, D. and Rudolph, J. (2006): Redox regulation of MAP kinase phosphatase 3. Biochemistry, **45**, 8476-8487.

Sugimoto, R., Kumagai, Y., Nakai, Y. and Ishii, T. (2005): 9,10-Phenanthraquinone in diesel exhaust particles downregulates Cu,Zn-SOD and HO-1 in human pulmonary epithelial cells: intracellular iron scavenger 1,10-phenanthroline affords protection against apoptosis. Free Radic. Biol. Med., **38**, 388-395.

Sun, Y., Sumi, D. and Kumagai, Y. (2006): Serine 1179 phosphorylation of endothelial nitric oxide synthase caused by 2,4,6-trinitrotoluene through PI3K/Akt signaling in endothelial cells. Toxicol. Appl. Pharmacol., **214**, 55-60.

Taguchi, K., Fujii, S., Yamano, S., Cho, A.K., Kamisuki, S., Nakai, Y., Sugawara, F., Froines, J.R. and Kumagai, Y. (2007): An approach to evaluate two-electron reduction of 9,10-phenanthraquinone and redox activity of the hydroquinone associated with oxidative stress. Free Radic. Biol. Med., **43**, 789-799.

Taguchi, K., Shimada, M., Fujii, S., Sumi, D., Pan, X., Yamano, S., Nishiyama, T., Hiratsuka, A., Yamamoto, M., Cho, A.K., Froines, J.R. and Kumagai, Y. (2008): Redox cycling of 9,10-phenanthraquinone to cause oxidative stress is terminated through its monoglucuronide conjugation in human pulmonary epithelial A549 cells. Free Radic. Biol. Med., **44**, 1645-1655.

Tiganis, T. (2002): Protein tyrosine phosphatases: dephosphorylating the epidermal growth factor receptor. IUBMB Life, **53**, 3-14.

Tonks, N.K. (2003): PTP1B: from the sidelines to the front lines! FEBS Lett., **546**, 140-148.

van Montfort, R.L., Congreve, M., Tisi, D., Carr, R. and Jhoti, H. (2003): Oxidation state of the active-site cysteine in protein tyrosine phosphatase 1B. Nature, **423**, 773-777.

Winterbourn, C.C. (1995): Toxicity of iron and hydrogen peroxide: the Fenton reaction. Toxicol. Lett., **82-83**, 969-974.

Zhang, W. and Liu, H.T. (2002): MAPK signal pathways in the regulation of cell proliferation in mammalian cells. Cell Res., **12**, 9-18.

Zhang, Z.Y. (1998): Protein-tyrosine phosphatases: biological function, structural characteristics, and mechanism of catalysis. Crit. Rev. Biochem. Mol. Biol., **33**, 1-52.

Zhang, Z.Y. (2003): Mechanistic studies on protein tyrosine phosphatases. Prog. Nucleic Acid Res. Mol. Biol., **73**, 171-220.

Zhang, Z.Y. and Dixon, J.E. (1993): Active site labeling of the Yersinia protein tyrosine phosphatase: the determination of the pKa of the active site cysteine and the function of the conserved histidine 402. Biochemistry, **32**, 9340-9345.